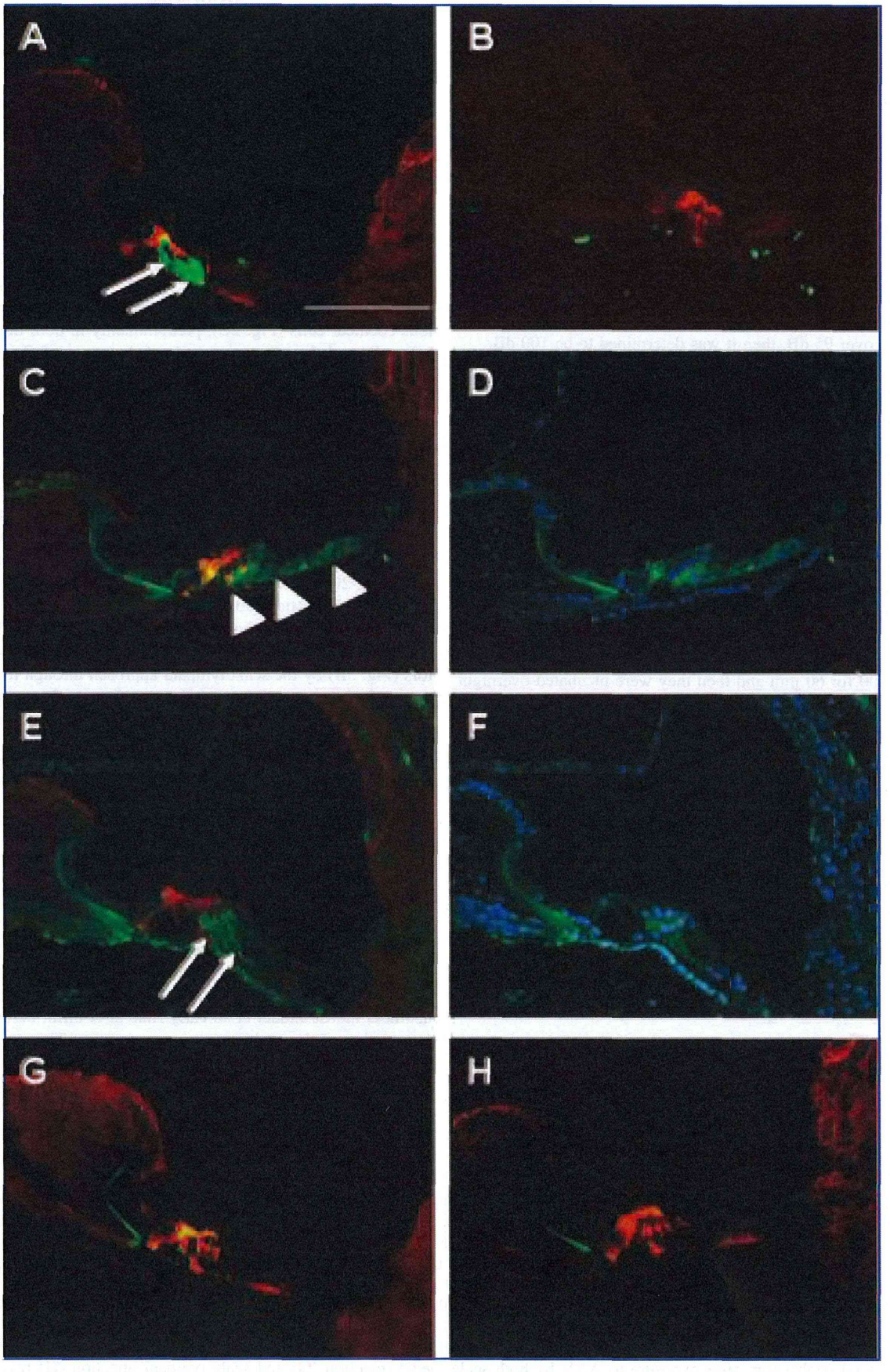

FIG. 2.

TABLE 1. EXPRESSION OF TRANSGENE IN MOUSE COCHLEAR CELLS

Vector	*Injection place*	*Total number*	*Inner hair cells*	*Outer hair cells*	*Pillar cells*	*Deiters cells*	*Hensen cells*	*Claudious cells*	*Inner sulcus cells*	*Outer sulcus cells*	*Stria vascularis*	*Spiral ganglion*	*Spiral ligament*	*Reissner's membrane*	*Spiral limbus*	*Mesothelial cells*
AAV	RW	$n = 6$	6	—	—	5	4	3	2	2	4	2	6	1	2	5
	Cochleostomy	$n = 6$	6	1	1	5	5	5	4	5	5	—	6	3	6	5
AdV	RW	$n = 5$	—	—	—	—	—	—	—	—	—	—	—	2	1	5
	Cochleostomy	$n = 3$	1	—	2	3	—	—	—	—	—	—	1	2	—	3

Abbreviations: AAV, adeno-associated virus; AdV, adenovirus; RW, round window.

[a]AAV or AdV was applied to the cochlea via the RW or cochleostomoy approach. Transgene expression the various cells of the inner ear was detected by the presence of green fluorescent protein.

[b]A dash (—) indicates no fluorescence in cells of the infected mouse cochlea.

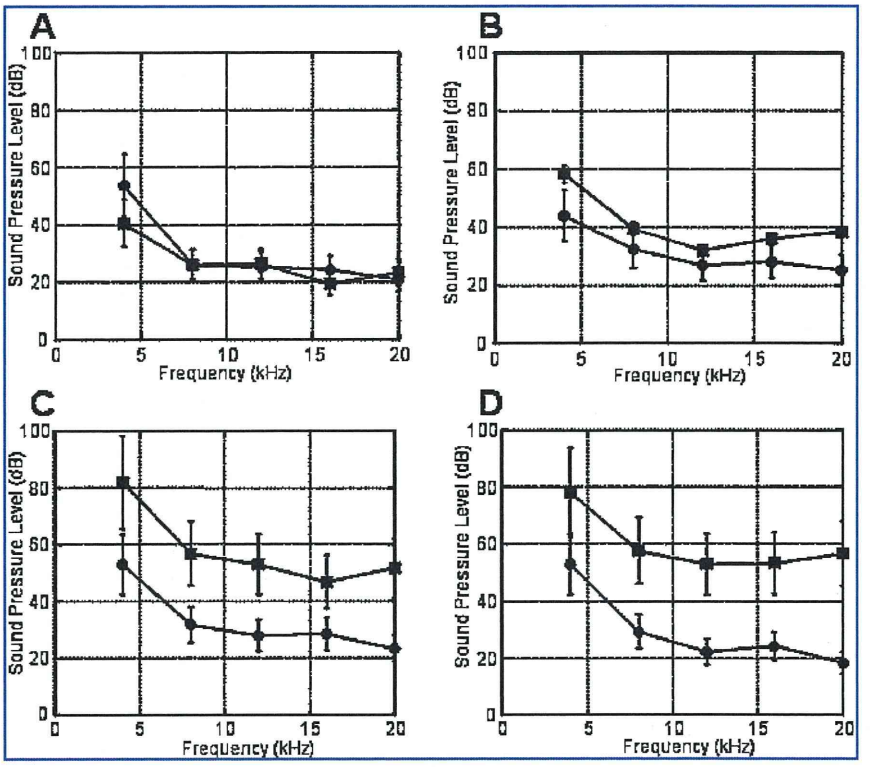

FIG. 3. ABR thresholds in mice after gene transfer. Threshold shifts at all frequencies were less than 15 dB in comparison with the contralateral side (*right*, solid circles) after the injection of AAV (**A**) or AdV (**B**) into the scala tympani (*left*, solid squares). On the other hand, injection of AAV (**C**) or AdV (**D**) into the scala media resulted in an elevation of ABR thresholds at all frequencies.

RW approach) and viral vector (AAV) for the neonatal mouse cochlea. The extent of AdV transfection was extremely limited in the mesenchymal cells, comparable to that obtained with adult mice; gene expression after AAV transfection by the RW approach was seen mainly in the cochlear supporting cells.

AAV serotype 1 was chosen on the basis of previously published reports indicating that AAV serotype 2 was unable to transduce hair cells or supporting cells of the cochlea either *in vivo* or *in vitro* (Kho *et al.*, 2000; Jero *et al.*, 2001a; Luebke *et al.*, 2001). There have been no reports demonstrating gene expression in supporting cells without hearing loss after injection into either the neonatal or adult mouse cochlea (Lalwani *et al.*, 1996, 1998; Jero *et al.*, 2001a; Luebke *et al.*, 2001; Duan *et al.*, 2002; Liu *et al.*, 2005, 2007).

When administering AdV in a cochlear organ culture, transgene expression was seen in most hair cells on P0 and in supporting cells on P3 to P5 (Kanzaki *et al.*, 2002). This study also demonstrates that AdV-mediated transgene expression was seen in both hair cells and supporting cells. On the other hand, transduction of P0 explants with AAV serotype 1 thus results in expression in the inner and outer hair cells, Hensen cells, and interdental cells (Stone *et al.*, 2005). In the present study, gene expression was also found mainly in supporting cells and inner hair cells on P0 *in vivo*, but not in supporting cells of the adult mouse as reported in previous studies. The difference in gene expression between adult and neonate may be explained in that supporting cells of the adult mouse do not have sialic acid on their surface as receptors for viral entry whereas those of the neonatal mouse do.

There are a number of genetic diseases that affect the cochlea early in life. *GJB2*, encoding gap junctional protein connexin26 (Cx26), which is expressed in supporting cells of the organ of Corti, is responsible for approximately half of all hereditary deafness cases (Kelsell *et al.*, 1997; Chang *et al.*, 2003). Animal models of both a conditional knockout of *Gjb2* (Cohen-Salmon *et al.*, 2002) and a dominant-negative *Gjb2* mutation (Kudo *et al.*, 2003) suggest that a critical but unknown function of the supporting cells is disturbed primarily by defective Cx26. Cx26 in the organ of Corti is extensively expressed in the mouse cochlea from birth (Frenz and Water, 2000; Zhang *et al.*, 2005). Furthermore, a dominant-negative *Gjb2* mutant mouse showed incomplete development of the cochlear supporting cells in our preliminary data. Thus, it is possible that the *Gjb2* mutation could be successfully treated by gene delivery to introduce the normal gene to the supporting cells of the neonatal cochlea.

In conclusion, this study has demonstrated excellent gene expression in supporting cells of the neonatal mouse cochlea, with good preservation of auditory function. It is therefore considered to be possible to repair hearing loss by applying the present method to the animal model of the *Gjb2* mutation, thereby suggesting the potential future effectiveness of such a modality for the development of gene-based therapies for humans.

ACKNOWLEDGMENTS

The authors thank Ms. J. Onoda, Mr. T. Yasuda, and Ms. T. Nihira for valuable technical assistance.

AUTHOR DISCLOSURE STATEMENT

No competing financial interests exist.

REFERENCES

CHANG, E.H., VAN CAMP, G., and SMITH, R.J. (2003). The role of connexins in human disease. Ear Hear. **24,** 314–323.

COHEN-SALMON, M., OTT, T., MICHEL, V., HARDELIN, J.P., PERFETTINI, I., EYBALIN, M., WU, T., MARCUS, D.C., WANGEMANN, P., WILLECKE, K., and PETIT, C. (2002). Target ablation of connexin26 in the inner ear epithelial gap junction network causes hearing impairment and cell death. Curr. Biol. **12,** 1106–1111.

DERBY, M.L., SENA-ESTEVES, M., BREAKEFIELD, X.O., and COREY, D.P. (1999). Gene transfer into the mammalian inner ear using HSV-1 and vaccine virus vectors. Hear. Res. **134,** 1–8.

DUAN, M.L., BORDET, T., MEZZINA, M., KAHN, A., and ULFENDAHL, M. (2002). Adenoviral and adeno-associated viral vector mediated gene transfer in the guinea pig cochlea. Neuroreport **13,** 1295–1299.

EISEN, M.D., and RYUGO, D.K. (2007). Hearing molecules: Contributions from genetic deafness. Cell. Mol. Life Sci. **64,** 566–580.

FRENZ, C.M., and WATER, T.R. (2000). Immunolocalization of connexin26 in the developing mouse cochlea. Brain Res. Rev. **32,** 172–180.

HAN, J.J., MHATRE, A.N., WAREING, M., PETTIS, R., ZUFFEREY, A.N., TRONO, D., and LALWANI, A.K. (1999). Transgene expression in the guinea pig cochlea mediated by the lentivirus-derived gene transfer vector. Hum. Gene Ther. **10,** 1867–1874.

ISHIMOTO, S., KAWAMOTO, K., KANZAKI, S., and RAPHAEL, Y. (2002). Gene transfer into supporting cells of organ of Corti. Hear. Res. **173,** 187–197.

JERO, J., MHATRE, A.N., TSENG, C.J., STERN, R.E., COLING, D.E., GOLDSTEIN, J.A., HONG, K., ZHENG, W.W., HOQUE, A.T.M.S., and LALWANI, A.K. (2001a). Cochlear gene delivery through an intact round window membrane in mouse. Hum. Gene Ther. **12,** 539–548.

JERO, J., TSENG, C.J., MHATRE, A.N., and LALWANI, A.K. (2001b). A surgical approach appropriate for targeted cochlear gene therapy in the mouse. Hear. Res. **151,** 106–114.

KANZAKI, S., OGAWA, K., CAMPER, S.A., and RAPHAEL, Y. (2002). Transgene expression in neonatal mouse inner ear explants mediated by first and advanced generation adenovirus vectors. Hear. Res. **169,** 112–120.

KANZAKI, S., SHIOTANI, A., INOUE, M., HASEGAWA, M., and OGAWA, K. (2007). Sendai virus vector-mediated transgene expression in the cochlea *in vivo*. Audiol. Neurotol. **12,** 119–126.

KAWAMOTO, K., OH, S.H., KANZAKI, S., BROWN, N., and RAPHAEL, Y. (2001). The function and structural outcome of inner ear gene transfer via the vestibular and cochlear fluids in mice. Mol. Ther. **4,** 575–585.

KELSELL, D.P., DUNLOP, J., STEVENS, H.P., LENCH, N.J., LIANG, J.N., PARRY, G., MUELLER, R.F., and LEIGH, I.M. (1997). Connexin26 mutations in hereditary non-syndromic sensorineural deafness. Nature **387,** 80–83.

KHO, S.T., PETTIS, R.M., MHATRE, A.N., and LALWANI, A.K. (2000). Safety of adeno-associated virus as cochlear gene transfer vector: Analysis of distant spread beyond injected cochleae. Mol. Ther. **2,** 368–373.

KUDO, T., KURE, S., IKEDA, K., XIA, A.P., KATORI, Y., SUZUKI, M., KOJIMA, K., ICHINOHE, A., SUZUKI, Y., AOKI, Y., KOBAYASHI, T., and MATSUBARA, Y. (2003). Transgenic expression of a dominant-negative connexin26 causes degeneration of the organ of Corti and non-syndromic deafness. Hum. Mol. Genet. **12,** 995–1004.

LALWANI, A.K., WALSH, B.J., REILLY, P.G., MUZYCZKA, N., and MHATRE, A.N. (1996). Development of *in vivo* gene therapy for hearing disorders: Introduction of adeno-associated virus into the cochlea of the guinea pig. Gene Ther. **3,** 588–592.

LALWANI, A.K., WALSH, B.J., REILLY, P.G., CARVALHO, G.J., ZOLOTUKHIN, S., MUZYCZKA, N., and MHATRE, A.N. (1998). Long-term *in vivo* cochlear transgene expression mediated by recombinant adeno-associated virus. Gene Ther. **5,** 277–281.

LIU, Y., OKADA, T., SHEYKHOLESLAMI, K., SHIMAZAKI, K., NOMOTO, T., MURAMATSU, S.I., KANAZAWA, T., TAKEUCHI, K., AJALLI, R., MIZUKAMI, H., KUME, A., ICHIMURA, K., and OZAWA, K. (2005). Specific and efficient transduction of cochlear inner hair cells with recombinant adeno-associated virus type 3 vector. Mol. Ther. **12,** 725–733.

LIU, Y., OKADA, T., NOMOTO T., KE X., KUME, A., OZAWA, K., and XIAO, S. (2007). Promoter effects of adeno-associated viral vector for transgene expression in the cochlea *in vivo*. Exp. Mol. Med. **39,** 170–175.

LUEBKE, A.E., FOSTER, P.K., MULLER, C.D., and PEEL, A.L. (2001). Cochlear function and transgene expression in the guinea pig cochlea, using adenovirus- and adeno-associated virus-directed gene transfer. Hum. Gene Ther. **12,** 773–781.

RAPHAEL, Y., FRISANCHO, J.C., and ROESSLER, B.J. (1996). Adenoviral-mediated gene transfer into guinea pig cochlear cells *in vivo*. Neurosci. Lett. **207,** 137–141.

SAMBROOK, J., and RUSSELL, D.W. (2001). Calcium-phosphate-mediated transfection of eukaryotic cells with plasmid DNAs. In: Irwin, N., and Janssen, K.A., eds. *Molecular Cloning: A Laboratory Manual*, 3rd ed. (Cold Spring Harbor Laboratory Press, New York) pp. 16.14–16.20.

STONE, I.M., LURIE, D.I, KELLEY, M.W., and POULSEN, D.J. (2005). Adeno-associated virus-mediated gene transfer to hair cells and support cells of the murine cochlea. Mol. Ther. **11,** 843–848.

SUZUKI, M., YAMASOBA, T., SUZUKAWA, K., and KAGA, K. (2003). Adenoviral vector gene delivery via the round window membrane in guinea pig. Neuroreport **14,** 1951–1955.

YAMADA, M., IWATSUBO, T., MIZUNO, Y., and MOCHIZUKI, H. (2004). Overexpression of α-synuclein in rat substantia nigra results in loss of dopaminergic neurons, phosphorylation of α-synuclein and activation of caspase-9: Resemblance to pathogenetic changes in Parkinson's disease. J. Neurochem. **91,** 451–461.

ZHANG, Y., TANG, W., AHMED, S., SIPP, J.A., CHEN, P., and LIN, X. (2005). Gap junction-mediated intercellular biochemical coupling in cochlear supporting cells is required for normal cochlear functions. Proc. Natl. Acad. Sci. U.S.A. **102,** 15201–15206.

Address reprint requests to:
Dr. Takashi Iizuka
Department of Otorhinolaryngology
Juntendo University School of Medicine
2-1-1 Hongo, Bunkyo-ku
Tokyo 113-8421, Japan

E-mail: t-iizuka@med.juntendo.ac.jp

Received for publication December 6, 2007; accepted after revision February 19, 2008.

Published online: March 26, 2008.

The American Journal of Pathology, Vol. 171, No. 1, July 2007

DOI: 10.2353/ajpath.2007.060948

Neurobiology

Mesenchymal Stem Cell Transplantation Accelerates Hearing Recovery through the Repair of Injured Cochlear Fibrocytes

Kazusaku Kamiya,* Yoshiaki Fujinami,* Noriyuki Hoya,* Yasuhide Okamoto,* Hiroko Kouike,* Rie Komatsuzaki,* Ritsuko Kusano,* Susumu Nakagawa,* Hiroko Satoh,† Masato Fujii,‡ and Tatsuo Matsunaga*

From the Laboratory of Auditory Disorders and Division of Hearing and Balance Research,‡ National Institute of Sensory Organs, and the Department of Plastic Surgery,† National Tokyo Medical Center, Tokyo, Japan*

Cochlear fibrocytes play important roles in normal hearing as well as in several types of sensorineural hearing loss attributable to inner ear homeostasis disorders. Recently, we developed a novel rat model of acute sensorineural hearing loss attributable to fibrocyte dysfunction induced by a mitochondrial toxin. In this model, we demonstrate active regeneration of the cochlear fibrocytes after severe focal apoptosis without any changes in the organ of Corti. To rescue the residual hearing loss, we transplanted mesenchymal stem cells into the lateral semicircular canal; a number of these stem cells were then detected in the injured area in the lateral wall. Rats with transplanted mesenchymal stem cells in the lateral wall demonstrated a significantly higher hearing recovery ratio than controls. The mesenchymal stem cells in the lateral wall also showed connexin 26 and connexin 30 immunostaining reminiscent of gap junctions between neighboring cells. These results indicate that reorganization of the cochlear fibrocytes leads to hearing recovery after acute sensorineural hearing loss in this model and suggest that mesenchymal stem cell transplantation into the inner ear may be a promising therapy for patients with sensorineural hearing loss attributable to degeneration of cochlear fibrocytes. ***(Am J Pathol 2007, 171:214–226; DOI: 10.2353/ajpath.2007.060948)***

Mammalian cochlear fibrocytes of the mesenchymal nonsensory regions play important roles in the cochlear physiology of hearing, including the transport of potassium ions to generate an endocochlear potential in the endolymph that is essential for the transduction of sound by hair cells.[1–3] It has been postulated that a potassium recycling pathway toward the stria vascularis via fibrocytes in the cochlear lateral wall is critical for proper hearing, although the exact mechanism has not been definitively determined.[2] One candidate model for this ion transport system consists of an extracellular flow of potassium ions through the scala tympani and scala vestibuli and a transcellular flow through the organ of Corti, supporting cells, and cells of the lateral wall.[4,5] The fibrocytes within the cochlear lateral wall are divided into type I to V based on their structural features, immunostaining patterns, and general location.[5] Type II, type IV, and type V fibrocytes resorb potassium ions from the surrounding perilymph and from outer sulcus cells via the Na,K-ATPase. The potassium ions are then transported to type I fibrocytes, strial basal cells, and intermediate cells through gap junctions and are secreted into the intrastrial space through potassium channels. The secreted potassium ions are incorporated into marginal cells by the Na,K-ATPase and the Na-K-Cl co-transporter, and are finally secreted into the endolymph through potassium channels.

Degeneration and alteration of the cochlear fibrocytes have been reported to cause hearing loss without any other changes in the cochlea in the Pit-Oct-Unc (POU)-domain transcription factor Brain-4 (Brn-4)-deficient mouse[6] and the otospiralin-deficient mouse.[3] *Brn-4* is the gene responsible for human DFN3, an X chromosome-linked nonsyndromic hearing loss. Mice deficient in Brn-4 exhibit reduced endocochlear potential and hearing loss and show severe ultrastructural alterations, including cel-

Supported by the Ministry of Health, Labor, and Welfare of Japan (health science research grant H16-kankakuki-006 to T.M.) and the Japan Foundation for Aging and Health (to K.K.).

Accepted for publication March 26, 2007.

Address reprint requests to Dr. Tatsuo Matsunaga, Laboratory of Auditory Disorders, National Institute of Sensory Organs (NISO), National Tokyo Medical Center, 2-5-1 Higashigaoka, Meguro-ku, Tokyo 152-8902, Japan. E-mail: matsunagatatsuo@kankakuki.go.jp.

lular atrophy and a reduction in the number of mitochondria, exclusively in spiral ligament fibrocytes.[6,7] In the otospiralin-deficient mouse, degeneration of type II and IV fibrocytes is the main pathological change, and hair cells and the stria vascularis appear normal.[3] Furthermore, in mouse and gerbil models of age-related hearing loss,[8–10] degeneration of the cochlear fibrocytes precede the degeneration of other types of cells within the cochlea, with notable pathological changes seen especially in type II, IV, and V fibrocytes. In humans, mutations in the connexin 26 (*Cx26*) and connexin 30 (*Cx30*) genes, which encode gap junction proteins and are expressed in cochlear fibrocytes and nonsensory epithelial cells, are well known to be responsible for hereditary sensorineural deafness.[11,12] These instances of deafness related to genetic, structural, and functional alterations in the cochlear fibrocytes highlight the functional importance of these fibrocytes in maintaining normal hearing.

Recently, we developed an animal model of acute sensorineural hearing loss attributable to acute cochlear energy failure by administering the mitochondrial toxin 3-nitropropionic acid (3NP) into the rat round window niche.[13,14] 3NP is an irreversible inhibitor of succinate dehydrogenase, a complex II enzyme of the mitochondrial electron transport chain.[15,16] Systemic administration of 3NP has been used to produce selective striatal degeneration in the brain of several mammals.[17,18] Our model with 3NP administration into the rat cochlea showed acute sensorineural hearing loss and revealed an initial pathological change in the fibrocytes of the lateral wall and spiral limbus without any significant damage to the organ of Corti or spiral ganglion. Furthermore, depending on the dose of 3NP used, these hearing loss model rats exhibited either a permanent threshold shift or a temporary threshold shift. In the present study, we used doses of 3NP that induce temporary threshold shift to explore the mechanism of hearing recovery after injury to the cochlear fibrocytes and examined a novel therapeutic approach to repair the injured area using mesenchymal stem cell (MSC) transplantation.

MSCs are multipotent cells that can be isolated from adult bone marrow and can be induced to differentiate into a variety of tissues *in vitro* and *in vivo*.[19] Human MSCs transplanted into fetal sheep intraperitoneally undergo site-specific differentiation into chondrocytes, adipocytes, myocytes, cardiomyocytes, bone marrow stromal cells, and thymic stroma.[20] Furthermore, when MSCs were transplanted into postnatal animals, they could engraft and differentiate into several tissue-specific cell types in response to environmental cues provided by different organs.[21] These transplantability features of MSCs suggested the possibility that they could restore hearing loss in 3NP-treated rats to the normal range. Recently, experimental bone marrow transplantation into irradiated mice suggested that a part of spiral ligament that consists of cochlear fibrocytes was derived from bone marrow cells or hematopoietic stem cells.[22] This indicates that bone marrow-derived stem cells such as MSCs may have a capacity to repair the injury of cochlear fibrocytes. In this study, we demonstrate that MSC transplantation significantly improves hearing recovery, and present evidence suggesting invasion of transplanted MSCs into the injured region of the cochlear lateral wall and repair of the interrupted gap junction network.

Materials and Methods

Rat Model of Acute Sensorineural Hearing Loss Attributable to Cochlear Fibrocyte-Specific Injury

Experimental procedures reported in this study were approved by the Institutional Animal Care and Use Committee of the National Tokyo Medical Center. Sprague-Dawley rats (Clea Japan, Tokyo, Japan) weighing between 180 and 210 g (8 to 10 weeks old) were used. Before surgery, the animals were anesthetized with pentobarbital (30 to 40 mg/kg, i.p.; Dainippon Pharmaceutical, Osaka, Japan), and after local administration of 1% lidocaine (AstraZeneca PLC, London, UK), an incision was made posterior to the left pinna near the external meatus. The left otic bulla was opened to approach the round window niche. The distal end of a section of PE 10 tubing (Becton-Dickinson, Franklin Lakes, NJ) was drawn to a fine tip in a flame and gently inserted into the round window niche. 3NP (Sigma, St. Louis, MO) was dissolved in saline at 300 mmol/L and the pH adjusted to 7.4 with NaOH. Saline alone was used as a control. The solution was administered for 2 minutes at a rate of 1.5 μl/minute with a syringe pump. After treatment, a small piece of gelatin was placed on the niche to keep the solution in the niche regardless of head movement, and the wound was closed. The right cochlea was surgically destroyed to avoid cross-hearing during auditory brainstem response (ABR) recording.

Auditory Brainstem Response

ABR recording was performed as previously described[13] before surgery and at 2 hours and 1, 2, 3, 7, 14, 21, 28, 35, and 42 days after surgery (or until 14 days in the MSC transplantation experiment). Six to 12 rats in each group were used for the recordings. ABR was recorded using Scope waveform storing and stimulus control software and the PowerLab data acquisition and analysis system (PowerLab2/20; AD Instruments, Castle Hill, Australia). Electroencephalogram recording was performed using a digital Bioamp extracellular amplifier system (BAL-1; Tucker-Davis Technologies, Alachua, FL). Sound stimuli were produced by a coupler type speaker (ES1spc; Bio Research Center, Nagoya, Japan) inserted into the ear canal. Pure tone bursts of 8, 20, and 40 kHz (0.2-ms rise/fall time and 1-ms flat segment) were generated, and the amplitude was specified by a real-time processor and programmable attenuator (RP2.1 and PA5; Tucker-Davis Technologies). Sound level calibration and frequency confirmation were performed using a 1/4 inch free-field mic (7016; ACO Pacific, Belmont, CA), microphone amp (MA3; Tucker-Davis Technologies), a digital oscilloscope (DS-8822P; Iwatsu Electronic, Tokyo, Japan), and a sound level meter (NL32; Rion, Tokyo, Japan). The maximum output level was 87, 86, and 96 dB at 8, 20, and 40

kHz, respectively. For recording, the animals were anesthetized with pentobarbital before stainless steel needle electrodes were placed ventrolateral to the ears. Waveforms of 512 stimuli at a frequency of 9 Hz were averaged, and the visual detection threshold was determined by increasing or decreasing the sound pressure level in 5-dB steps. The effects of 3NP and/or MSC transplantation on the ABR threshold and recovery ratio of ABR threshold (peak threshold − threshold at 14 days or 42 days/peak threshold × 100) were statistically analyzed at each frequency using an unpaired Student's *t*-test. The significance level for all statistical procedures was set at $P < 0.05$.

Bromodeoxyuridine (BrdU) Injection

To detect cell proliferation in the rat inner ear, BrdU (Sigma) was injected (30 mg/kg i.p. per single injection) as previously described.[23] Injections were started just after 3NP administration and continued every 12 hours for 3 or 6 days.

MSC Preparation

We previously established bone marrow MSCs and demonstrate their potential to differentiate into several cell types.[24] The cells were prepared from 6- to 8-week-old male F344 rats (Clea) as described. In brief, surgical treatment was performed after intraperitoneal injection of pentobarbital (30 to 40 mg/kg, i.p.). After surgery, the rats were sacrificed by ether inhalation followed by dislocation of the neck. Rat femurs and tibiae were collected and the long bones meticulously dissected to remove all adherent soft tissue. Both ends of the bones were cut away from the diaphyses with bone scissors. The bone marrow plugs were hydrostatically expelled from the bones by inserting 18-gauge needles fastened to 10-ml syringes filled with complete medium [Dulbecco's modified Eagle's medium (Sigma), 10% fetal bovine serum (Sigma), and 100 U/ml penicillin-streptomycin (Sigma)] into the distal ends of the femora and the proximal ends of the tibiae. Cells were plated on plastic culture dishes. The nonadherent cell population was removed after 24 hours, and the adherent layer was washed once with fresh media. The cells were then continuously cultured for 1 to 4 weeks in complete medium. Medium was completely replaced every 3 days. When the cells were nearly confluent, the adherent cells were released from the dishes with 0.25% trypsin-ethylenediaminetetraacetic acid (Sigma), split 1:3, and seeded onto fresh plates. Cells from passages 10 to 15 were stored with Cell Banker reagent (Juji Field, Tokyo, Japan) in liquid nitrogen. The frozen cell suspensions were thawed at 1 week before the transplantation and cultured in complete medium at 37°C in a humidified atmosphere of 5% CO_2. The potential of these cells as MSCs were previously demonstrated as described.[24] The surface marker expression of these cells was analyzed by flow cytometry (Epics Altra with HyPerSort cell sorting system; Beckman Coulter, Fullerton, CA). At ~80 to 90% confluence, MSCs were dissociated by treatment with 1× Accutase (Chemicon International, Temecula, CA) for 15 minutes at 37°C followed by phosphate-buffered saline (PBS) washout, centrifugation at 1200 rpm for 10 minutes, and resuspension in Hanks' balanced salt solution $(HBSS)^+$ medium [$HBSS^-$ medium (Invitrogen Japan, Tokyo, Japan) with 2% fetal bovine serum and 10 mmol/L 2-[4-(2-hydroxyethyl)-1-piperazinyl]ethanesulfonic acid (HEPES) buffer (Invitrogen Japan)]. MSCs were incubated with antibodies against CD45, CD31, CD29, CD44H, CD54, CD73, and CD90 (BD PharMingen, San Diego, CA) for 30 minutes on ice and spun down. At the end of the staining, MSCs were resuspended in ice-cold $HBSS^+$ medium containing 2 μg/ml propidium iodide for discrimination of dead cells. To detect the MSCs after injection, cultured MSCs were incubated with 5 μmol/L BrdU for 2 days before transplantation as previously described.[25]

MSC Transplantation

Before transplantation, cultured MSCs were released from the dishes with 0.25% trypsin-ethylenediaminetetraacetic acid and washed by centrifugation with Dulbecco's phosphate-buffered saline (D-PBS; Invitrogen Japan) and resuspended to prepare MSC suspension (1×10^5 cells in 20 μl of D-PBS) for the following transplantation. Three days after 3NP administration, the rats were anesthetized with pentobarbital (30 to 40 mg/kg, i.p.) and by local administration of 1% lidocaine. Incisions were made as described for 3NP administration, the surfaces of the posterior and lateral semicircular canals were exposed, and a small hole was made in each canal. A small tube (Eicom, Kyoto, Japan) was inserted into the lateral semicircular canal toward the ampulla. Through this tube, the perilymph was perfused with an MSC suspension (1×10^5 cells in 20 μl of D-PBS) for 10 minutes at a rate of 2 μl/minute using a syringe pump with drainage from the hole made on the posterior semicircular canal. The tube was then removed, the holes on the semicircular canals were sealed with a muscle and fibrin adhesive (Beriplast P Combi-set; CSL Behring, King of Prussia, PA), and the wound on the neck was closed. An equal volume of vehicle (D-PBS) was also injected into the semicircular canal of 3NP-treated rats as control.

Tissue Preparation

The rats were sacrificed at 3 days (three rats for 3NP and three rats for saline control) and 42 days (five rats for 3NP and three rats for saline control) after 3NP treatment and 11 days after MSC transplantation (12 rats for 3NP with MSC transplantation, seven rats for MSC transplantation only, and five rats for 3NP followed by vehicle injection). They were deeply anesthetized with pentobarbital and transcardially perfused with 0.01 mol/L phosphate buffer, pH 7.4, containing 8.6% sucrose followed by a fixative consisting of freshly depolymerized 4% paraformaldehyde in 0.1 mol/L phosphate buffer (pH 7.4). After decapitation, the left temporal bones were removed and immediately placed in the same fixative. Small openings

were made at the round window, oval window, and the apex of the cochlea. After overnight immersion in fixative, the temporal bones were decalcified by immersion in 5% sucrose, 5% ethylenediaminetetraacetic acid, pH 7.4, with stirring at 4°C for 14 days. The specimens were dehydrated through graded concentrations of alcohol, embedded in paraffin blocks, and sectioned into 5-μm-thick slices. The sections were stained with hematoxylin and eosin (H&E) as generally described, by terminal deoxynucleotidyl transferase (TdT)-mediated dUTP nick-end labeling (TUNEL) and by immunohistochemistry for BrdU, Cx30, or Cx26 as described below.

TUNEL Assay

TUNEL assays were performed using an ApopTag Fluorescein Direct *in situ* apoptosis detection kit (Chemicon International) according to the manufacturer's instructions. In brief, specimens were digested with 20 μg/ml proteinase K in 0.01 mol/L PBS, pH 7.4, for 5 minutes, incubated with TdT and fluorescein-labeled nucleotide in a humid atmosphere at 37°C for 1 hour, and then incubated with 2 μmol/L TOPRO-3 iodide (Molecular Probes, Eugene, OR) for 5 minutes. The specimens were viewed with a confocal laser microscope (LSM510; Carl Zeiss, Esslingen, Germany; or Radiance 2100; Bio-Rad, Hercules, CA), and each image was analyzed and saved by ZeissLSM image browser (Carl Zeiss). Negative controls included proteinase K digestion but did not include TdT so that nonspecific incorporation of nucleotide, or nonspecific binding of enzyme-conjugate, could be assessed. Distilled water was substituted for TdT enzyme reagent in negative controls.

Immunohistochemistry

After pretreatment with 2 mol/L HCl at 37°C for 30 minutes, incubation with 20 μg/ml proteinase K in PBS for 5 minutes, and incubation with blocking solution (1.5% normal goat serum in PBS) for 30 minutes at room temperature, tissue sections were incubated with anti-BrdU antibody (DAKO, Glostrup, Denmark) diluted 1:100 in PBS for 30 minutes, then with biotin-conjugated anti-mouse IgG (Vector, Burlingame, CA) diluted 1:200 in PBS for 30 minutes, followed by horseradish peroxidase (HRP)-conjugated streptavidin-biotin complex (streptABComplex-HRP, Vectastain Elite ABC kit standard; Vector) for 1 hour at room temperature. Sections were stained in DAB-H_2O_2 (Vector) for 3 minutes and hematoxylin for 1 minute and then rinsed and covered with a coverslip. For BrdU and TUNEL double staining, Alexa568-conjugated anti-mouse IgG (1:600; Molecular Probes) was used as a secondary antibody in the BrdU staining after the TUNEL procedure. For double-staining of BrdU with Cx30 or Cx26, rabbit anti-Cx26 (1:300; Zymed Laboratories, South San Francisco, CA) or rabbit anti-Cx30 (1:400; Zymed Laboratories) antibody and anti-BrdU antibody were used as a primary antibody cocktail, and Alexa488-conjugated anti-rabbit IgG (1:400; Molecular Probes) with Alexa568-conjugated anti-mouse IgG were used as a secondary antibody cocktail. For nuclear staining, TO-PRO-3 iodide (2 μmol/L; Molecular Probes), 4,6-diamidino-2-phenylindole (1 μg/ml; Dojindo Laboratories, Kumamoto, Japan) or propidium iodide (1 μg/ml; Molecular Probes) was used. Negative controls were performed without primary antibodies to assess nonspecific binding of the secondary antibody or of the streptAB-Complex-HRP. Inner ear sections that were not injected with BrdU were also used as negative controls. Background autofluorescence was not observed in the cochlear sections with the tissue preparation methods used in the present study.

Results

Long-Term Observation of Temporary Threshold Shift and Hearing Recovery after 3NP Administration

We monitored ABR thresholds in 3NP-treated rats at 8, 20, and 40 kHz for 42 days after 3NP administration (Figure 1, A–C) to examine the potential for hearing recovery. At all frequencies, the ABR thresholds peaked 1 day after 3NP administration and then gradually recovered. At 8 kHz (n = 7), the threshold reached within a normal threshold level (11 dB) 42 days after 3NP administration. However, the ABR threshold at 40 kHz showed only a mild recovery after 14 days. The hearing recovery ratio, which is described in Materials and Methods, was calculated for each tested frequency (Figure 1D). At 14 days, the recovery ratios were 73.4 ± 5.5% for 8 kHz (n = 11), 57.0 ± 11.2% for 20 kHz (n = 11), and 37.5 ± 7.7% for 40 kHz (n = 12). At 42 days, they were 97.2 ± 9.4% for 8 kHz (n = 7), 67.0 ± 16.4% for 20 kHz (n = 7), and 32.3 ± 7.7% for 40 kHz (n = 7). Throughout the recovery time course, the recovery ratios at the lower frequencies always tended to be higher than those at the highest frequency. At 42 days, the recovery ratio for 8 kHz was significantly higher than that for 40 kHz (P = 0.005). Between 14 and 42 days after 3NP administration, the hearing level for 40 kHz did not show significant recovery, but the recovery ratios for 8 and 20 kHz showed 24 and 10% increases, respectively.

Apoptosis and Regeneration of the Cochlear Fibrocytes after 3NP Administration

To analyze the pathological changes associated with the acute hearing loss observed in the 3NP-treated rats, we performed H&E staining and TUNEL reaction to detect apoptosis. No histological changes were observed in the organ of Corti and spiral ganglion of rats with 3NP administration as shown in Figure 2, A and B. However, severe apoptosis, with chromatin condensation and apoptotic bodies, was observed only in the lateral wall and the spiral limbus at 3 days after 3NP administration (Figure 2, C and D). These severe apoptotic regions included more than 30% TUNEL-positive or apoptotic cells and were clearly demarcated as shown in Figure 2,

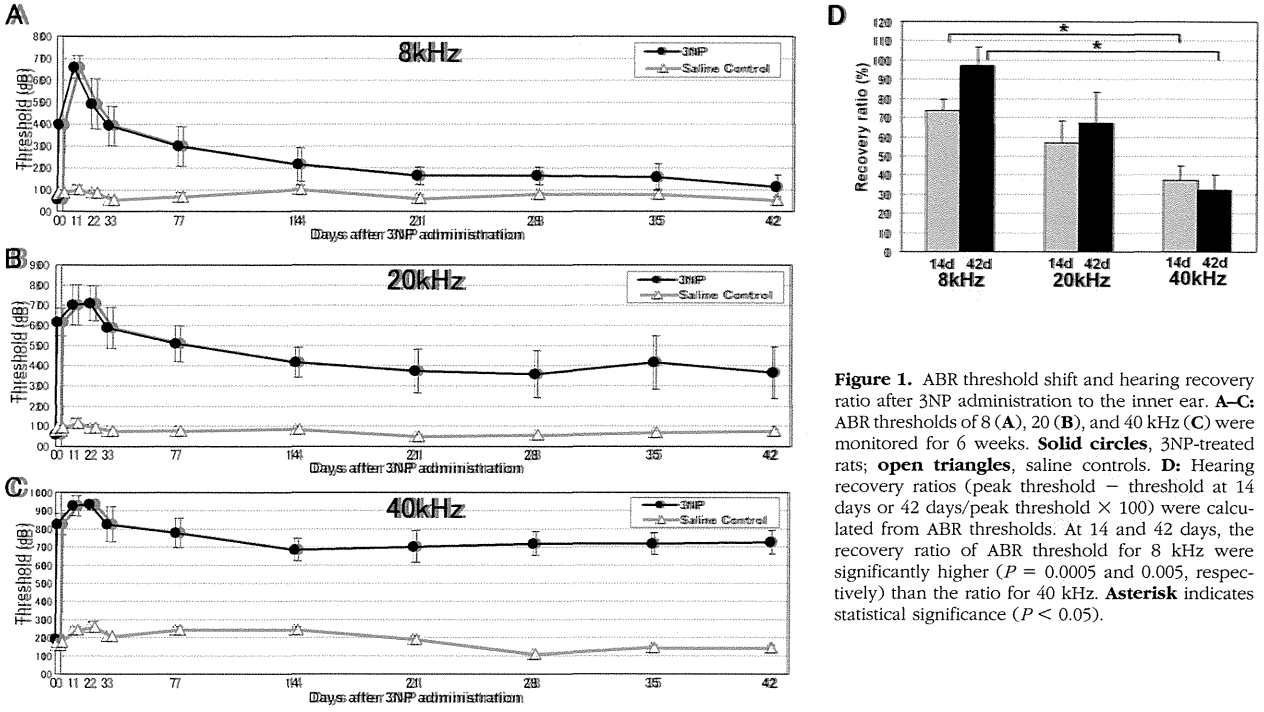

Figure 1. ABR threshold shift and hearing recovery ratio after 3NP administration to the inner ear. **A–C:** ABR thresholds of 8 (**A**), 20 (**B**), and 40 kHz (**C**) were monitored for 6 weeks. **Solid circles**, 3NP-treated rats; **open triangles**, saline controls. **D:** Hearing recovery ratios (peak threshold − threshold at 14 days or 42 days/peak threshold × 100) were calculated from ABR thresholds. At 14 and 42 days, the recovery ratio of ABR threshold for 8 kHz were significantly higher ($P = 0.0005$ and 0.005, respectively) than the ratio for 40 kHz. **Asterisk** indicates statistical significance ($P < 0.05$).

E and F. These areas contain cochlear fibrocytes that participate in the potassium recycling route within the cochlea. The typical distribution pattern of TUNEL-positive cells after 3NP treatment is shown in Figure 2E, but a few rats with more severe hearing impairment (with ~55 dB elevation of the ABR threshold) demonstrated more prominent histological changes, with focal cell loss in the center surrounded by TUNEL-positive cells (Figure 2, G and H). On light microscopic observation of H&E-stained sections, histological changes suggesting inflammation were not evident in the lateral wall and spiral limbus. As for cochlear turns, lateral wall in basal turn had more severe damage than the middle turn as shown in Figure 4, G, I, and J, and the apical turn had little damage in the lateral wall.

To analyze the mechanism of hearing recovery after damage to the cochlear lateral wall, we performed a BrdU incorporation assay in addition to the TUNEL assay (Figure 3). BrdU-positive cells were observed mainly in the lateral wall fibrocytes and occasionally observed in spiral limbus, Schwann cells, and Reissner's membrane. At 3 days after 3NP administration, the BrdU-positive cell count around the area of apoptosis in the lateral wall was 6.2 ± 0.7 cells (19 cross sections from three rats) compared with 0.5 ± 0.1 cells (12 cross sections from three rats) for the control (Figure 3, A–C). Furthermore, a few TUNEL-positive dying cells that take up BrdU were detected, indicating that some fibrocytes that regenerated after 3NP administration also became apoptotic 3 days after 3NP administration (Figure 3C, arrow). To trace the cells regenerated after the early injury, the rats were continuously injected with BrdU during the first 6 days after 3NP administration and sacrificed 42 days after 3NP administration for detection of BrdU-positive cells. Few TUNEL-positive cells were detected, but a number of BrdU-positive cells could be detected in the central part of the lateral wall in the middle turn of the cochlea (Figure 3, D–F). At 42 days after 3NP administration, 2.6 ± 0.8 BrdU-positive cells were detected in a cross section of the lateral wall of the middle turn in 3NP-treated rats (26 cross sections from five rats) compared with 0.2 ± 0.2 cells in saline-treated controls (12 cross sections from three rats). In contrast, only a few BrdU-positive cells were detected in the spiral limbus at 3 and 42 days after 3NP administration.

Characterization of MSCs

For the MSC transplantation into inner ear, we used rat bone marrow-derived cells, which we previously established and demonstrated their capacity for differentiation as MSC.[24] Flow cytometry of these MSCs before the transplantation demonstrated surface expression of CD29, CD44H, CD54, CD73, and CD90, but not of CD31 or CD45. This surface expression pattern was similar to human and murine MSCs.[26,27]

Transplantation and Detection of MSCs in the Inner Ear Tissue

To improve the hearing recovery of high-frequency (40 kHz) sounds, we transplanted BrdU-labeled MSCs into the inner ear of 3NP-treated rats using perilymphatic perfusion with MSC suspension from the lateral semicircular canal. Eleven days after transplantation, a number of BrdU-positive cells were observed along the ampullary crest surface facing the perilymph in the lateral semicircular canal that was closest to the site of MSC injection (Figure 4A, arrow), suggesting that the transplanted

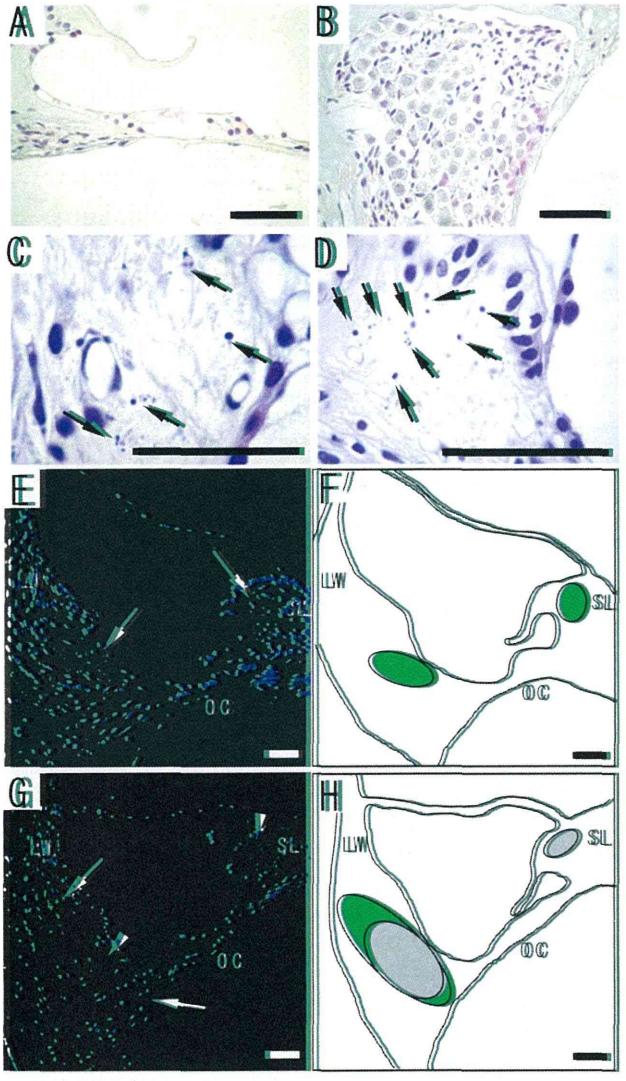

Figure 2. Apoptosis in the rat cochlea at 3 days after 3NP administration. **A–D:** H&E staining of the cochlea. Severe focal apoptosis showing chromatin condensation and apoptotic bodies (**arrows**) was observed in the lateral wall (**C**) and the spiral limbus (**D**), whereas no morphological changes were observed in the organ of Corti (**A**) and the spiral ganglion (**B**). **E** and **G:** TUNEL staining (green) of the cochlea in rats showing moderate (~35 dB elevation of ABR threshold for 8 kHz, **E**) and severe (~55 dB elevation of ABR threshold for 8 kHz, **G**) hearing impairment. **E:** The areas of apoptosis indicated by TUNEL-positive cells (**arrows**) were clearly demarcated in the lateral wall and spiral limbus. Nuclei were stained by TOPRO-3. **G:** Acellular areas (**arrowheads**) corresponded to the apoptotic areas in **E**, and severe apoptosis was observed in the area around the acellular site (**arrows**). Schematic illustration of the areas of apoptosis and cell loss in **E** and **G** are shown in **F** and **H**, respectively. Areas of apoptosis including more than 30% of TUNEL-positive cells or apoptotic cells are indicated in green, and areas of loss of fibrocytes are indicated in gray. SL, spiral limbus; LW, lateral wall; OC, organ of Corti. Scale bars = 50 μm.

MSCs survived there even 11 days after injection. Some of these BrdU-positive cells were attached to the surface of the ampullary crest (Figure 4B, asterisk) and a number of cells had invaded the tissue (Figure 4B, arrow) although a few of the invading cells displayed morphological features suggesting rejection by the host tissue. Aggregations of MSCs were frequently observed on the bone surface in the scala tympani (Figure 4, C and D). In the apical part of the lateral wall facing the scala vestibuli, a number of BrdU-positive cells were detected within the tissue (Figure 4E). These cells showed the morphological features of pretransplantation MSCs, ie, large and round (Figure 4F). Many BrdU-positive cells were also observed in the middle part of the lateral wall (Figure 4G) injured by 3NP treatment. The shape of these MSCs resembled that of the cochlear fibrocytes. In the hook region of the cochlea, a large number of BrdU-positive cells were also detected in the area neighboring the lateral wall injury (Figure 4, H and I). In the lateral wall of the middle turn, BrdU-positive cells were occasionally observed without a loss of fibrocytes in the corresponding area, suggesting that the MSCs that had invaded the lateral wall supplemented the injured area to repair damage (Figure 4J). In contrast to the lateral wall, only a few BrdU-positive cells were detected in the spiral limbus (Figure 4K, arrow). No morphological changes were observed in any cochlear hair cells in every group.

We used 12 3NP-treated rats and seven nontreated rats for BrdU-labeled MSC transplantation. BrdU-positive cells were detected in all of the inner ear tissues of the examined rats. Successful invasion of the lateral wall by MSCs was observed in 6 of the 12 rats treated with 3NP and one of the seven control rats (Table 1). Thus, the rats with lateral wall injury had a higher rate of MSC invasion of the lateral wall than those without injury. BrdU-positive cells were counted in five cross sections of the cochlear middle turn in each rat that showed invasion of MSCs into the lateral wall after 3NP and MSC treatment, and the approximate mean values of BrdU-positive cells observed in a cross section of the cochlear middle turn distributed between 11 and 15 in scala tympani, between 6 and 10 in apical part of lateral wall, middle part of lateral wall, and scala vestibuli, less than one in spiral limbus, and not detected in the organ of Corti and the spiral ganglion.

Expression of Gap Junction Proteins in Transplanted MSCs

To investigate the functional contribution of MSCs detected in injured and uninjured areas of the lateral wall, we analyzed expression of the gap junction proteins Cx30 and Cx26 in the transplanted MSCs. Gap junctions between cochlear fibrocytes play an important role in the cochlear potassium recycling system, and breaks in the gap junction network because of loss of fibrocytes are thought to be a main cause of the 3NP-induced hearing loss. In both normal and 3NP-treated rats, both Cx30 and Cx26 had the same expression pattern in most fibrocytes of the whole part of the lateral wall. Immunostaining for Cx30 or Cx26 showed punctuate cytoplasmic staining and strong spots of staining mainly at the sites of attachment to adjacent fibrocytes (Figure 5, A–L). All of the MSCs invaded into the lateral wall showed the expression of Cx30 and Cx26. The expression patterns of Cx30 and Cx26 in cochlear fibrocytes were the same between apical part and middle part of lateral wall, but only the invaded MSCs in the apical part of lateral wall showed different expression patterns. The MSCs detected in the apical part also expressed Cx30 and Cx26; however,